

Journal of Materials Chemistry C

Accepted Manuscript



This is an *Accepted Manuscript*, which has been through the Royal Society of Chemistry peer review process and has been accepted for publication.

Accepted Manuscripts are published online shortly after acceptance, before technical editing, formatting and proof reading. Using this free service, authors can make their results available to the community, in citable form, before we publish the edited article. We will replace this *Accepted Manuscript* with the edited and formatted *Advance Article* as soon as it is available.

You can find more information about *Accepted Manuscripts* in the [Information for Authors](#).

Please note that technical editing may introduce minor changes to the text and/or graphics, which may alter content. The journal's standard [Terms & Conditions](#) and the [Ethical guidelines](#) still apply. In no event shall the Royal Society of Chemistry be held responsible for any errors or omissions in this *Accepted Manuscript* or any consequences arising from the use of any information it contains.

ARTICLE

Multiple horizontal-dip-coating of small molecular emission layers for solution-processable organic light-emitting devices

Cite this: DOI: 10.1039/x0xx00000x

Hong Goo Jeon and Byoungchoo Park*

Received 00th January 2014,

Accepted 00th January 2014

DOI: 10.1039/x0xx00000x

www.rsc.org/

We report an investigation of small molecular organic light-emitting diodes (SM-OLEDs) which consist of solution-processable light-emitting layers (EMLs) fabricated using a horizontal-dip (H-dip-)coating method. The EMLs used were composed of a co-mixed small molecular host matrix of hole-transporting 4,4',4''-tris(N-carbazolyl)-triphenylamine and electron-transporting 2,7-bis(diphenyl phosphoryl)-9,9'-spirobifluorene, doped with blue-, green-, and red-emitting iridium phosphors. To investigate the film-forming ability, the film quality levels of H-dip-coated small molecular EMLs with multiple coatings were observed while increasing the number of coating cycles. It was found that the thickness of the EML increases as the number of cycles of H-dip-coating increases. Moreover, the formation of film defects in the form of nano-pinholes in the EMLs was found to decrease dramatically with an increase in the number of H-dip-coating cycles. By applying three H-dip-coatings of EML solutions, highly homogeneous small molecular EMLs were successfully deposited, demonstrating that the use of the triple-H-dip-coated EMLs in SM-OLEDs results in good device performance, with maximum luminance levels of 25,000 cd m⁻², 79,000 cd m⁻², and 15,000 cd m⁻², with corresponding peak current efficiencies of 15.8 cd A⁻¹, 23.2 cd A⁻¹, and 5.7 cd A⁻¹, for blue-, green, and red SM-OLEDs, respectively. These results clearly indicate that H-dip-coated EMLs with multiple coatings will yield bright and efficient all-solution-processable SM-OLEDs.

Introduction

Numerous recent studies have focused on the development of organic and polymeric semiconducting materials and related device structures for use in organic light-emitting diodes (OLEDs), in order to realise cost-efficient, lightweight, flexible, and large-area flat panel displays and solid state lighting applications.¹⁻⁵ In order to achieve such aims, the developments of particular interest to researchers are the improved device performance, stability, and simplicity of the device fabrication process. In respect of the device performance of OLEDs, for example, their internal quantum efficiency has already been significantly improved to nearly 100% due to the incorporation of phosphorescent guest dopants into the emission layers (EMLs), which leads to strong spin-orbit coupling and a rapid intersystem crossing, resulting in an efficient radiative transition from the triplet states to a ground state.³⁻⁶ The use of such electrophosphorescent iridium complexes has enabled the demonstration of phosphorescent OLEDs with a relatively high

peak luminescence range of *ca.* 50,000-100,000 cd m⁻² and peak efficiency that exceeds 25 cd A⁻¹.^{4,5}

In general, such electrophosphorescent small-molecular OLEDs (SM-OLEDs) can be divided into two classes: those prepared by vacuum-evaporation deposition³⁻¹² and those fabricated by solution-processing methods such as spin-coating and blade-coating.¹³⁻²² Researchers have tended to use the complicated co-vacuum-evaporation deposition of multiple components to fabricate multi-layered SM-OLEDs, as the performances of vacuum-deposited SM-OLEDs have been superior to those of solution-processed devices thus far.³⁻¹² Nevertheless, in comparison with vacuum-evaporation, which can be used to create complex structures but which wastes a large amount of organic material and incurs relatively high fabrication costs, solution-processing techniques are particularly appealing due to their potential advantages of a larger area, a simpler process, and cost-effective manufacturing.¹³⁻¹⁶

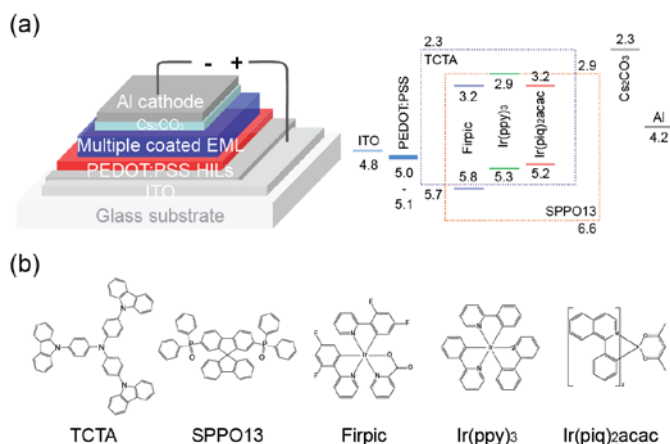


Fig. 1 (a) The device configurations of the solution-processable small molecular OLEDs studied together with the relevant energy level diagrams, and (b) chemical structures of the materials used in the EMLs.

Recently, several important studies of phosphorescent SM-OLEDs fabricated by solution-processing methods have been reported.^{16–22} In one proposed method, mixed hosts consisting of hole- and electron-transporting small molecular materials are employed to improve the charge balance and increase the size of the recombination zone in solution-processed SM-OLEDs.^{16–20} For example, it was reported that a solution-coated SM-OLED containing green phosphors as doped emitters exhibits good EL performances, with a peak efficiency of 56.9 cd A⁻¹ achieved.¹⁸ In most such solution-processed mixed-host SM-OLEDs, EMLs with precise ratios of multiple components of mixed hosts/doped guest emitters (host/guest) have generally been fabricated by a spin-coating method. With a spin-coating technique, EMLs can be simply formed on substrates. However, limitations with respect to the coating area and the inhomogeneous morphology of spin-coated EMLs may prevent solution-coating methods from being used in high-throughput manufacturing.^{22–24} Hence, despite all of these successes, including recent developments in the solution-processing of SM-OLEDs, a simple and reliable solution-processing technique for small molecular EMLs in SM-OLEDs holds some attraction in view of the ability of such a method to form flat and uniform layers over a large area given its potential advantages with regard to the production of simple and cost-effective SM-OLEDs. The further development of a viable, alternative solution-coating process for small-molecular EMLs, together with the design of a novel device structural framework capable of providing high-performance SM-OLEDs, is therefore necessary in order to fabricate solution-processable SM-OLEDs.

In this study, we fabricated and investigated solution-processable blue, green, and red SM-OLEDs based on solution-processable small molecular EMLs using commercial materials, as shown in Fig. 1. For the solution-processable blue-emitting small molecular EMLs, we chose 4,4',4''-tris(N-carbazolyl)-triphenylamine (TCTA, the first-triplet energy level (T1): 2.73 eV)¹⁸ as the hole-transporting host and 2,7-bis(diphenylphosphoryl)-9,9'-spirobifluorene (SPPO13, lowest unoccupied molecular orbital (LUMO): ~2.78 eV)¹⁸ as an electron-transporting host of co-mixed-host materials (TCTA:SPPO13) doped with the phosphor bis[2-(4,6-difluorophenyl) pyridinato-C2,N] (picolinato) iridium(III) (Firpic, LUMO: 2.9–3.2 eV, highest occupied molecular orbital (HOMO): 5.8 eV, T1: 2.65 eV).^{17,18} We also used the green-

emitting phosphor tris(2-phenylpyridinato) iridium (Ir(ppy)₃, LUMO: 2.92 eV, HOMO: 5.32 eV, T1: 2.9 eV)¹³ and the red-emitting phosphor bis(1-(phenyl)isoquinoline) iridium acetylacetonate (Ir(piq)₂acac, LUMO: 3.23 eV, HOMO: 5.17 eV, T1: 2.0 eV)¹¹ as co-guests in EMLs during the fabrication of the solution-processed SM-OLEDs. In order to improve the film-forming ability as well as the EL performance of the EMLs, we used the well-known, advanced coating method known as horizontal dip- (H-dip-) coating.^{23–27} The H-dip-coating technique creates effective coatings of organic, polymeric, and inorganic semiconducting layers. Extensions of H-dip-coating include solution-coating methods for large OLEDs,^{23,24} polymer solar cells,^{24–26} and semiconducting layers for organic thin-film transistors.²⁷ The advantage of H-dip-coating is that the coating thickness is easily controlled by external parameters. By applying multiple H-dip-coatings of EML solutions, we obtained highly homogeneous and defect-free small molecular EMLs. SM-OLEDs based on the triple-H-dip-coated EMLs exhibited good device performance levels with maximum luminance levels of 25,000 cd m⁻², 79,000 cd m⁻², and 15,000 cd m⁻² with peak current efficiencies of 15.8 cd A⁻¹, 23.2 cd A⁻¹, and 5.7 cd A⁻¹ for blue-, green, and red SM-OLEDs, respectively. We attribute this good device performance to the multiple H-dip-coatings, which provided good film-forming ability. We also demonstrate the feasibility of the simple fabrication of solution-processed EMLs in SM-OLEDs using multiple-H-dip-coated EMLs, showing considerable promise as a mass-produced alternative to vacuum-evaporated layers.

Experimental

Materials. The hole-injection material poly(styrene sulfonic acid) doped poly(3,4-ethylenedioxythiophene) (PEDOT:PSS, CLEVIOS™ P VP AI 4083, H.C. Starck) was used as received from the manufacturer. For solution-processable EML, the hole-transporting material TCTA (Lumtec), the electron-transporting material SPPO13 (Lumtec), the blue-emitting phosphor Firpic (Lumtec), the green-emitting phosphor Ir(ppy)₃ (Lumtec), and the red-emitting phosphor Ir(piq)₂acac (Lumtec) were used as received without further purification. The electron-injection material of Cs₂CO₃ (Sigma-Aldrich) and the cathode of Al (Sigma-Aldrich) were also used as received. The chemical structures of the materials used are shown in Fig. 1(b).

H-dip-coatings. The apparatus we used for the H-dip-coating process had a maximum work space of 10 cm × 10 cm (see Fig. 2(a)). A small volume of solution (~5–10 μl) per unit of coating area (1 cm × 1 cm) was fed into the gap of the cylindrical H-dip-coating head (SUS steel) using a syringe pump (New Era Pump Systems Inc., NE-1000). The height of the gap h_0 was adjusted vertically using two micrometer positioners mounted at either end of the coating head, and the carrying speed U was controlled by a computer-controlled translation stage (SGSP26-200, Sigma Koki Co., Ltd). After a meniscus of coating solution had formed on the substrate, the substrate was transported horizontally such that the H-dip-coating head spread the solution evenly on the transporting substrate while maintaining the shape of the downstream meniscus of the solution. The transporting speed U was set to 1.5 cm s⁻¹, and it took approximately 1 min to prepare a film on a substrate with a length of about 1 m.

Device fabrication. As shown in Fig. 1(a), the solution-processed SM-OLEDs were fabricated on glass substrates pre-coated with an 80 nm layer of indium tin oxide (ITO) that had a sheet resistance of 30 Ω per square. The ITO substrates were ultrasonically cleaned

with detergent, deionised water, acetone and isopropanol, in that sequence, after which they were dried by blowing nitrogen over them, followed by ultra-violet ozone cleaning for 15 min. A 40-nm hole-injection layer (HIL) of PEDOT:PSS was H-dip-coated onto the pre-cleaned ITO substrates and then baked at 120 °C in a vacuum oven for 10 min to extract any residual water. The PEDOT:PSS solution used was a mixture of a PEDOT:PSS solution (1%) and isopropyl alcohol with a weight ratio of 2:1. Next, to fabricate the blue SM-OLEDs, a well-mixed emissive solution for EMLs was prepared using the mixed solvents 1,2-dichloroethane and chloroform (at a mixing weight ratio of 3:1) by dissolving co-mixed hosts consisting of TCTA and SPPO13 and the phosphorescent blue-emitter Firpic as a guest. The mixed host was TCTA:SPPO13 with 48% SPPO13, and the concentration of Firpic was maintained at 17% (optimised for blue emission). Afterwards, the EMLs were also H-dip-coated subsequently on top of the PEDOT:PSS HIL from the mixed emissive solution and then annealed at 110 °C in a vacuum oven for 5 min to remove any residual solvent; the thickness of the EMLs was approximately 80 nm. Then, an electron-injecting interfacial layer of Cs₂CO₃ (2 nm) and an Al cathode layer (*ca.* 50 nm) were formed sequentially on top of the EML via thermal deposition at a rate of 0.2 nm s⁻¹ under a base pressure of 2 × 10⁻⁶ Torr. The overlap between the ITO and Al electrodes was 3 mm × 3 mm as the active emissive area of the devices. It is important to note that the fabrication process of the green and red guests of Ir(ppy)₃ and Ir(piq)₂acac can be utilised with mixed blue EML solutions when making green and red SM-OLEDs. The concentrations of Ir(ppy)₃ and Ir(piq)₂acac were 0.15 and 0.07 wt% in the green and red SM-OLEDs, respectively.

Characterization. The optical properties of the fabricated functional layers were investigated using an UV-vis spectrometer (Thermo Scientific Ltd.). In order to investigate the surface morphologies of the fabricated layers, variations in the surface roughness levels of the layers were monitored using an atomic force microscope (AFM, Nanosurf Easyscan 2 AFM, Nanosurf AG Switzerland Inc.). The current density-luminance-voltage (*J-L-V*) characteristics and the Commission Internationale d'Éclairage (CIE) chromatic coordinates were measured using a Keithley source measurement unit (Keithley 2400) and a luminance meter (Chroma Meter CS-200, Konica Minolta Sensing, Inc.). The EL spectra were measured using a spectrometer (Ocean's Optics), and an integrating sphere measurement system (LCS-100, SphereOptics Inc.) was used to measure the emission characteristics. The characterization of the device was carried out at room temperature under ambient conditions, without encapsulation.

Results and discussion

Multiple-H-dip-coated small molecular EMLs for solution-processable OLEDs

Figure 2(a) shows a schematic illustration of the H-dip-coating method²³⁻²⁷ used in this study for solution-processable SM-OLEDs. With the H-dip-coating process, the thickness of the layer can be controlled precisely because it increases with an increase in the capillary number ($C_a = \mu U / \sigma$) of the coating solution, where μ and σ represent the viscosity and surface tension of the coating solution, respectively, and U is the coating speed. The film thickness (h) of the H-dip-coated layer can be described by the associated drag-out problem proposed by Landau and Levich for the condition of $C_a \ll 1$; $h = k \cdot C_a^{2/3} \cdot R_d$, where R_d represents the radius of the associated downstream meniscus and k is a constant for proportionality.²³⁻

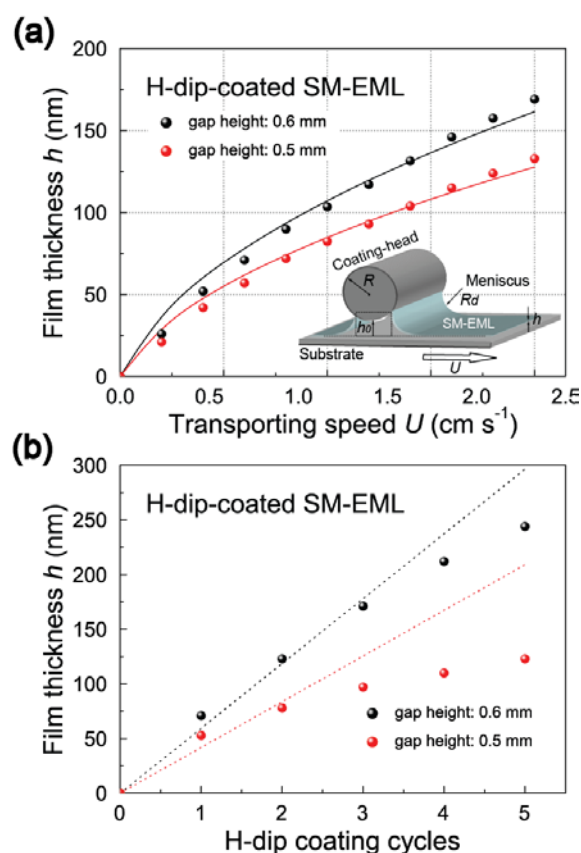


Fig. 2 (a) Coated film thickness data of the small molecular blue EML as a function of the carrying speed U for the two gap heights denoted by h_0 . The solid curves show the theoretically fitted predictions by the Landau-Levich equation. The inset shows a schematic illustration of the H-dip-coating process with gap height h_0 and coating speed U . (b) Coated film thickness data of the small molecular blue EML as functions of the number of H-dip-coating cycles at a carrying speed U of 2.0 cm s⁻¹ for two gap heights h_0 .

²⁸ We initially investigated the thickness of the H-dip-coated EML as a function of the coating speed U and the gap height h_0 (Fig. 2(a)). As shown in the figure, for an h_0 value of 0.5 mm, the film thickness of the H-dip-coated EML showed a continuous increase from *ca.* 25 nm to *ca.* 125 nm when U was increased from 0.25 to 2.0 cm s⁻¹. Furthermore, when h_0 was increased to 0.6 mm, the thickness of the H-dip-coated EML continued to increase with U . These results were in good agreement with the theoretical description of the associated drag-out problem (the solid curves in Fig. 2(a)).

Next, we investigated the thickness of the H-dip-coated EMLs as a function of the number of H-dip-coating cycles (Fig. 2(b)). As shown in the figure, for an h_0 value of 0.5 mm, the film thickness of the H-dip-coated EML increased from *ca.* 50 nm to *ca.* 125 nm when the number of H-dip-coating cycles was increased from 1 to 5. Furthermore, when h_0 was increased to 0.6 mm, the thickness of the H-dip-coated EML also increased in keeping with the number of coating cycles. It is thus clear that multiple coatings with the H-dip-coating process can offer precise control of the thicknesses of EMLs of small molecules using not only U and h_0 but also the number of coating cycles as controlling parameters, in contrast to the

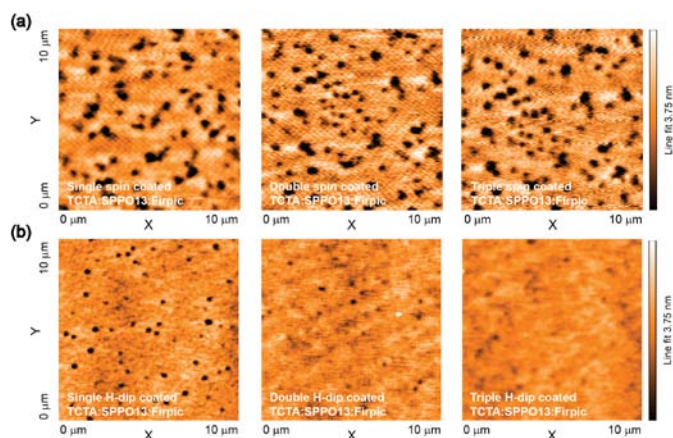


Fig. 3 (a) $10\ \mu\text{m} \times 10\ \mu\text{m}$ AFM topography images of the spin-coated (a) and H-dip-coated (b) blue small molecular EMLs of TCTA:SPPO13:Firpic for different coating cycles: (left) one cycle, (middle) two cycles, and (right) three cycles.

conventional spin-coating method, which can easily destroy the formed underlying layers.

Film quality of the multiple-H-dip-coated small molecular EMLs

Next, in order to investigate the film quality of the small molecular EMLs, we monitored the variation in the surface roughness of the H-dip-coated EMLs using AFM. Figure 3 shows the AFM morphologies of spin-coated and H-dip-coated EMLs (thickness: 80 nm) of blue-emitting TCTA:SPPO13:Firpic deposited on top of flat substrates with different coating cycles, i.e., with one cycle, two cycles, and three cycles. As shown in the figure, because multiple instances of spin-coating re-dissolved the underlying layers that were pre-coated on the substrate when the same solvents were used, low-quality and inhomogeneous EMLs were formed by the multiple-spin-coating process. The investigation showed that the topography became rough as the number of coating cycles increased; the root-mean-square (RMS) surface roughness of an EML fabricated by single spin-coating was *ca.* 0.73, while the RMS surface roughness of EMLs fabricated by double spin-coating and triple spin-coating were *ca.* 0.89, and 0.85 nm, respectively. Moreover, the small molecular EMLs of TCTA:SPPO13:Firpic fabricated by spin-coating showed sub-micron-sized pinhole defects down to the nano-pore level, which could deteriorate the device performance. For H-dip-coating, as shown in Fig. 3 (b), the small molecular EML of TCTA:SPPO13:Firpic fabricated by single H-dip-coating showed a similar surface morphology with many sub-micron-sized pinhole defects down to the nano-pore level and a relatively high surface roughness (*ca.* 0.50 nm). On the other hand, in contrast to the multiple-spin-coated EMLs, the multiple-H-dip-coated TCTA:SPPO13:Firpic EMLs were of good quality even when the same solvents were used. These investigations showed that the topographies of the EMLs fabricated by multiple H-dip-coating became more homogeneous as the number of coating cycles was increased; the RMS surface roughness levels of EMLs fabricated by double H-dip-coating and triple H-dip-

coating were *ca.* 0.40, and 0.30 nm, respectively, even for the same film thickness (80 nm) of each EML fabricated. Moreover, no pinhole defects or instances of phase separation could be observed in the multi-component small molecular EMLs fabricated by triple H-dip-coating (Fig. 3 (b)), and the surface roughness of the EML was identical at different positions for the layers investigated. This uniformity was achieved because the conditions under which the EMLs were formed involved the rapid film coating action of H-dip-coating before re-dissolving the underlying layers, unlike the conventional spin-coating method. The resulting smooth and uniform EMLs of TCTA:SPPO13:Firpic provide a clear indication that the layers

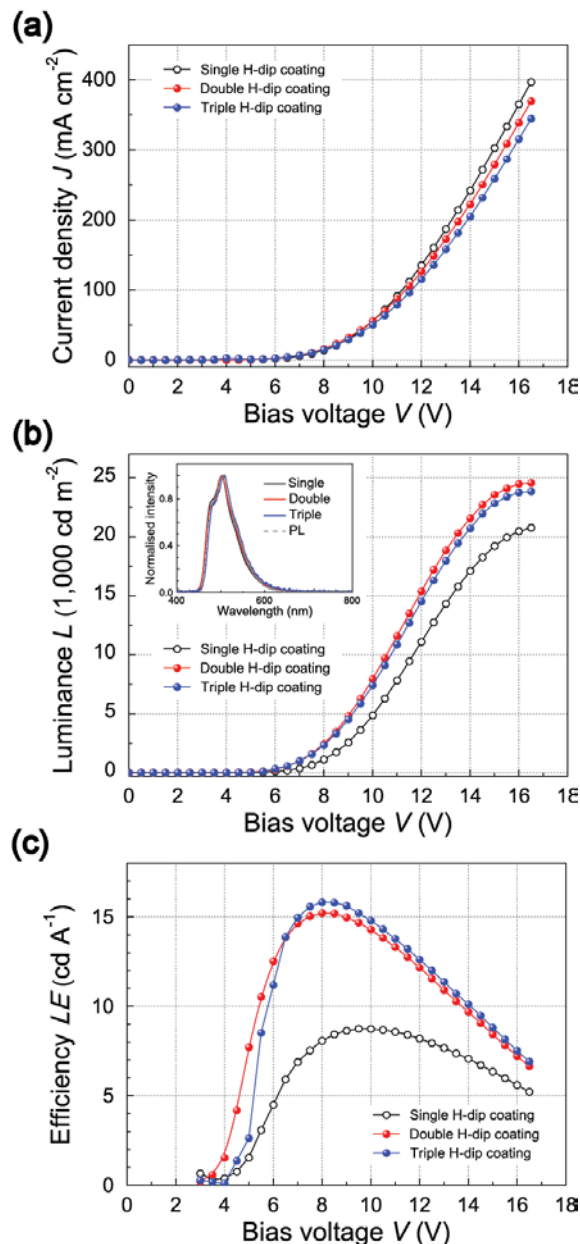


Fig. 4 (a) Current density-voltage (J - V), (b) luminance-voltage (L - V), and (c) luminance efficiency-voltage (LE - V) characteristics of blue SM-OLEDs including multiple-H-dip-coated EMLs of the TCTA:SPPO13:Firpic system. The inset in (b) shows the normalised PL and EL spectra obtained from the blue SM-OLEDs studied here.

fabricated by multiple H-dip-coating may be suitable for the fabrication of solution-processed SM-OLEDs.

Solution-processable SM-OLEDs based on the multiple-H-dip-coated EMLs of co-mixed host:guest systems

Given the impressive film quality levels of the EMLs fabricated by multiple H-dip-coating, we fabricated blue SM-OLEDs including EMLs of the co-mixed TCTA:SPPO13 host and the blue-emitting Firpic phosphor guest. For the blue SM-OLEDs, blue devices of [ITO anode/ PEDOT:PSS HIL / multiple-H-dip-coated TCTA:SPPO13:Firpic EML (80 nm) / Cs₂CO₃ electron-injecting buffer layer / Al cathode] were fabricated. For comparison, a reference device with a single-H-dip-coated EML was also fabricated. Here, the blue OLEDs were optimised with a thickness of 80 nm for the EML. When the thickness of the EML was changed from 80 nm, the device performance began gradually to deteriorate.

In order to estimate the effect of number of H-dip-coating cycles for the TCTA:SPPO13:Firpic EMLs with regard to device performance levels, we investigated the current density-voltage-luminance (*J-L-V*) characteristics of the fabricated blue SM-OLEDs, as shown in Fig. 4. For all of the OLEDs, the slopes of the *J-V* curves between 0 and 16.5 V indicated excellent diodic behaviour of the H-dip-coated EMLs (Fig. 4(a)). It is also clear from the *J-L-V* curves (Figs. 4(a) and (b)) that the charge injections are below 4.0 V, with sharp increases in the *J-L-V* curves above this range. For example, the operating voltage of the reference SM-OLED with the single-H-dip-coated EML is about 6.0 V for a brightness of 100 cd m⁻²; it is 8.0 V for 1,000 cd m⁻² and 12.0 V for 10,000 cd m⁻². The luminescence reached ca. 21,000 cd m⁻² (at 16.5 V). The figure also shows that the blue EL brightness levels increase significantly in the devices with the multiple-H-dip-coated EMLs. The operating voltage of the SM-OLED with the triple-H-dip-coated EML is about 5.5 V for a brightness of 100 cd m⁻²; it is 7.0 V for 1,000 cd m⁻² and 11.0 V for 10,000 cd m⁻². The luminescence reached ca. 25,000 cd m⁻² (at 16.5 V). The increased EL brightness indicates that excitons are efficiently generated by the introduction of the multiple-H-dip-coated EMLs, which may cause an increase in the number of radiative exciton recombinations via the electron-hole balance in the EMLs.¹⁶⁻²⁰ A possible mechanism for the efficient formation of excitons is the reduction of unbalanced electron or hole current flows in multiple-H-dip-coated EMLs caused by the good coverage without film defects or phase separation for the multiple-H-dip-coated EMLs. The inset in Fig. 4(b) shows the normalised EL spectra (at 1,000 cd m⁻²) obtained from blue SM-OLEDs with multiple-H-dip-coated EMLs. As shown in the figure, characteristic dominant peaks are observed at 480-500 nm for the blue devices, corresponding to the EL emission from Firpic.^{18,29}

Interestingly, it was also noted that the efficiencies increase significantly when the multiple-H-dip-coated EMLs are introduced (Fig. 4(c)); the best overall performance is obtained in a blue device with triple-H-dip-coated EMLs, where a peak

luminance efficiency (*LE*) of 15.8 cd A⁻¹ and a peak power efficiency (*PE*) of 6.7 lm W⁻¹ are achieved. Even at a luminance level of 10,000 cd m⁻², the *LE*s of blue devices with double- and triple-H-dip-coated EMLs reach 13.8 and 13.7 cd A⁻¹, respectively, which are higher than that (8.2 cd A⁻¹) of the reference device with the single-H-dip-coated EML. Moreover, the external quantum efficiencies (*EQEs*) of blue devices with double- and triple-H-dip-coated EMLs are 4.7% and 5.3%, respectively, which are also higher than that (3.9%) of the reference device with the single-H-dip-coated EML. These results clearly indicate that the device performance levels are significantly improved when multiple-H-dip-coated EMLs are used. Note that the device performance is optimised with three coating cycles. When the number of coating cycles for the EMLs exceeds three, the device performance starts to become saturated. These results show that the introduction of multiple-H-dip-coated EMLs into small molecular blue OLEDs readily produces bright and efficient blue SM-OLEDs. The performances of the blue devices studied here are summarised in Table 1.

As shown above, it is clear that when the number of H-dip-coating cycles increases, there are significant increases in EL performance levels. In order to understand this improvement in the EL performance, we investigated the depth distributions of the mixed components in the EMLs, which may be also related

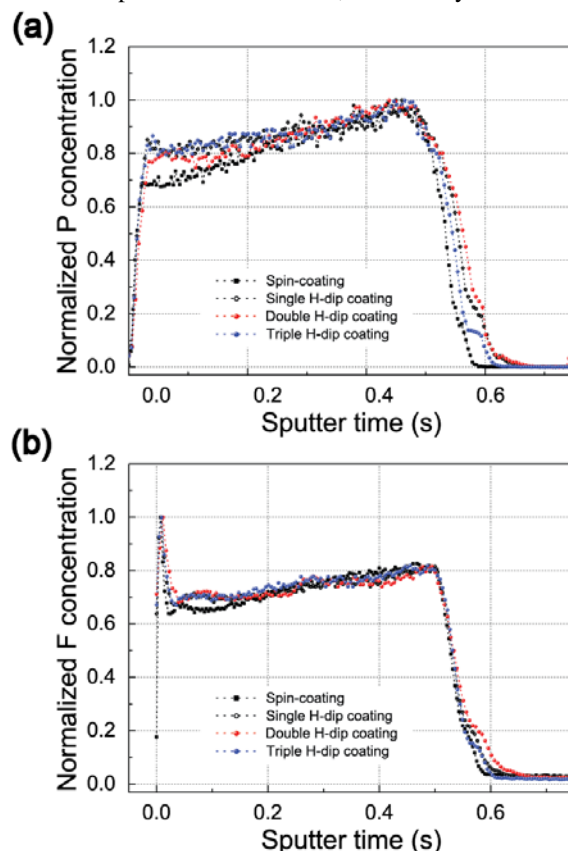


Fig. 5 ToF-SIMS depth profiles of phosphorus (P) (a) and fluorine (F) (b) ions in blue-emissive SM-OLEDs with multiple-H-dip-coated and spin-coated EMLs of TCTA:SPPO13:Firpic. A sputter time of zero was used on the top surfaces of the devices.

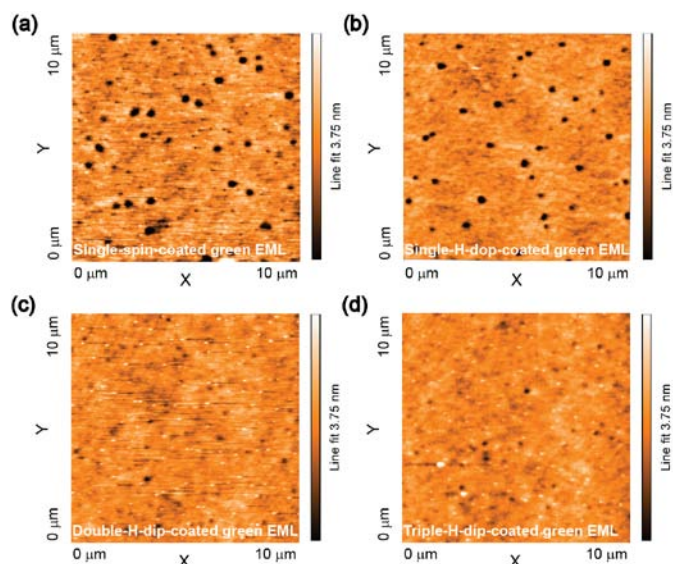


Fig. 6 10 $\mu\text{m} \times 10 \mu\text{m}$ AFM topography images of spin-coated (a) and H-dip-coated green small molecular EMLs of TCTA:SPPO13:Firpic:Ir(ppy)₃ for different coating cycles: (b) one cycle, (c) two cycles, and (d) three cycles.

to the EL performance of the devices,^{30,31} using time-of-flight secondary ion mass spectrometry (ToF-SIMS).³² Figure 5 shows depth profiles of phosphorus (P in only SPPO13) and fluorine (F in only Firpic) ions in the EMLs of the multiple-H-dip-coated blue SM-OLEDs. As shown in the figure, the depth profiles of P and F ions in the multiple-H-dip-coated EMLs are nearly identical to those of the single-H-dip-coated EML, while those in the spin-coated EMLs are slightly different. Thus, the improved EL performance of multiple-H-dip-coated EMLs cannot be explained in terms of changes in the vertical depth distribution of mixed components in H-dip-coated EMLs. These SIMS results therefore indicate that the improved device performance of the sample device is mainly caused by the formation of homogeneous EMLs without any defects in them, although further systematic studies of EL performance characteristics are necessary to understand the fundamental processes underlying the charge-transport and recombination phenomena.

The foregoing results clearly demonstrate that multiple-H-dip-coated blue EMLs of the co-host:guest system can be used to fabricate bright and efficient solution-processable blue SM-OLEDs. It is also important to note that the solution-process approach using multiple instances of H-dip-coating is more convenient than conventional vacuum-evaporation for fabricating multi-component EMLs considering that the desired compositions of the EMLs can easily be achieved by the appropriate weighting of the components, in preference to the more complicated co-evaporation process.

Next, we fabricated and investigated green SM-OLEDs including multiple-H-dip-coated EMLs of the co-mixed TCTA:SPPO13 host and co-mixed guest phosphors of Firpic:Ir(ppy)₃. Figure 6 shows the AFM morphologies of the spin-coated and H-dip-coated EMLs (thickness: 80 nm) of green-emitting TCTA:SPPO13:Firpic:Ir(ppy)₃ deposited onto

flat substrates with different coating cycles, i.e., one cycle, two cycles, and three cycles. As shown in the figure, similar to the blue-emitting EMLs, the small molecular EMLs of TCTA:SPPO13:Firpic:Ir(ppy)₃ fabricated by spin-coating and by single H-dip-coating also showed surface morphologies with many sub-micron-sized pinhole defects and relatively high surface roughness levels (*ca.* 0.64 nm). In contrast to these single-H-dip-coated EMLs, multiple-H-dip-coated TCTA:SPPO13:Firpic:Ir(ppy)₃ EMLs exhibited good film-forming abilities. This investigation also showed that the topographies of the EMLs fabricated by multiple H-dip-coating became more homogeneous as the number of H-dip-coating

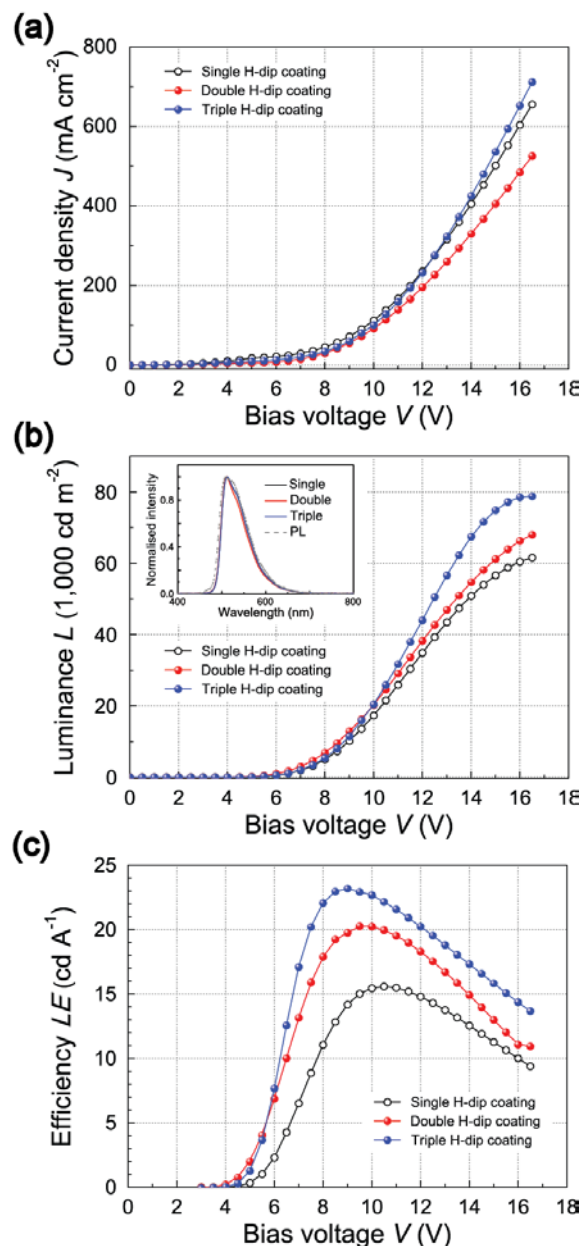


Fig. 7 J - V (a), L - V (b), and (c) LE - V characteristics of multiple-H-dip-coated green SM-OLEDs based on co-mixed EMLs of TCTA:SPPO13:Firpic:Ir(ppy)₃. The inset in (b) shows the normalised PL and EL spectra obtained from the green SM-OLEDs studied here.

cycles increased; the RMS surface roughness levels of EMLs fabricated by double H-dip-coating and triple H-dip-coating were *ca.* 0.38, and 0.34 nm, respectively. Moreover, defects such as pinholes and/or phase separation were not found in these multi-component small molecular EMLs created by triple H-dip-coating. In addition, the surface roughness characteristics of the EMLs were identical at different positions for the layers investigated.

We also investigated the *J-L-V* characteristics of the multiple-H-dip-coated green SM-OLEDs, as shown in Fig. 7. For all of these OLEDs, the slopes of the *J-V* curves between 0 and 16.5 V indicate excellent diodic behaviour of the H-dip-coated EMLs. It is also clear from the *J-L-V* curves that the charge injections are below 4.0-4.5 V, with sharp increases in the *J-L-V* curves above this range; for example, the operating voltage of the green SM-OLED with the single-H-dip-coated EML is approximately 5.5 V for a brightness level of 100 cd m⁻²; it is also 6.5 V for 1,000 cd m⁻² and 9.0 V for 10,000 cd m⁻². Finally, the luminescence could go as high as *ca.* 62,000 cd m⁻² (at 16.5 V). The figure also shows that the green EL brightness levels increased significantly in the devices with the multiple-H-dip-coated EMLs. A peak luminance of 79,000 cd m⁻² was achieved in the green device with the triple-H-dip-coated EMLs. This level is much higher than that of the device with the single-H-dip-coated EML. Moreover, it was also noted that the efficiency levels were significantly increased when multiple-H-dip-coated EMLs are introduced. The best overall performance was obtained in the green device with the triple-H-dip-coated EMLs, with a peak luminance efficiency (*LE*) of 23.2 cd A⁻¹ and a peak power efficiency (*PE*) of 8.7 lm W⁻¹. Even at a luminance level of 10,000 cd m⁻², the *LE*s of green devices with double- and triple-H-dip-coated EMLs still reach 19.7 and 23.2 cd A⁻¹, respectively, which are higher than that (14.2 cd A⁻¹) of

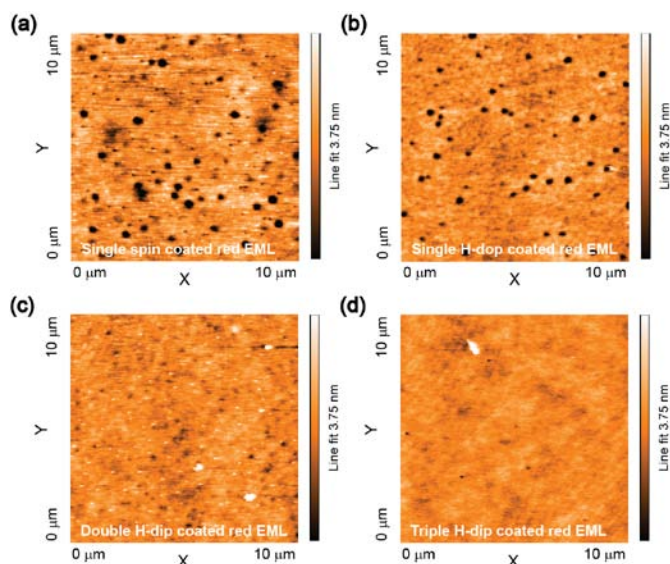


Fig. 8 10 μm × 10 μm AFM topography images of spin-coated (a) and H-dip-coated red small molecular EMLs of TCTA:SPPO13:Firpic:Ir(ppy)₃:Ir(piq)₂acac for different coating cycles: (b) one cycle, (c) two cycles, and (d) three cycles.

the device with the single-H-dip-coated EML. Moreover, the EQEs of green devices with double- and triple-H-dip-coated EMLs are 7.6% and 8.2%, respectively, which are also higher than that (7.1%) of the reference device with the single-H-dip-coated EML. These results clearly indicate that the device performance levels are significantly improved when multiple-H-dip-coated EMLs are used. The inset in Fig. 7(b) shows the normalised EL spectra (at 1,000 cd m⁻²) obtained from the green OLEDs with multiple-H-dip-coated EMLs. As shown in the figure, only single dominant peaks exist at 520 nm for the green devices, corresponding to the emission from Ir(ppy)₃.¹³ The performance levels of the green devices studied are

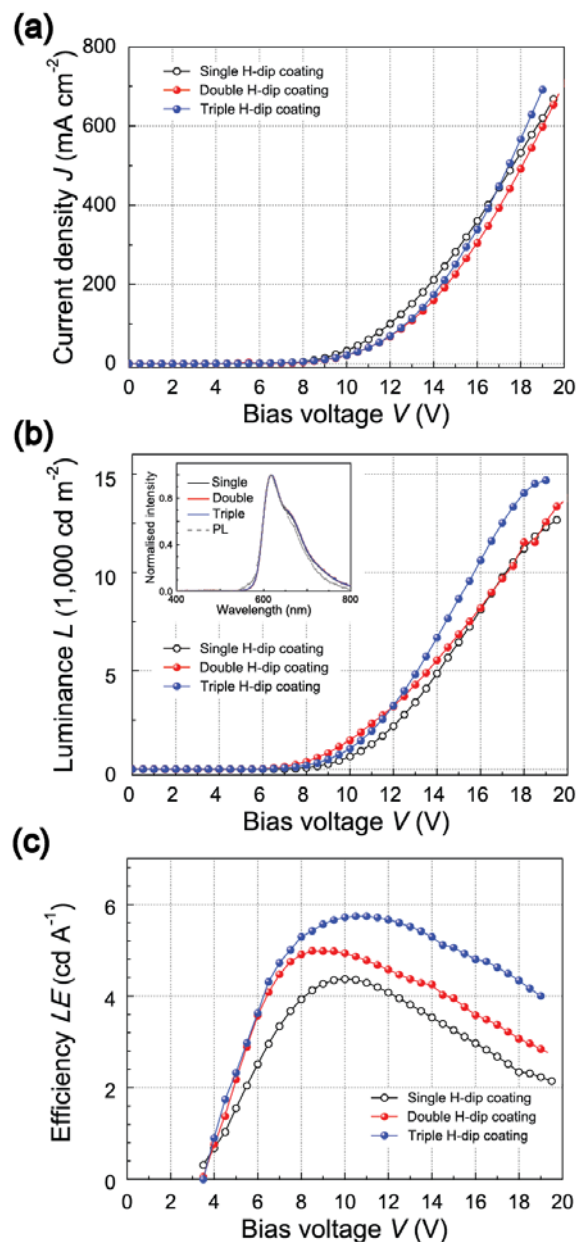


Fig. 9 *J-V*, (b) *L-V*, and (c) *LE-V* characteristics of multiple-H-dip-coated red SM-OLEDs based on co-mixed EMLs of TCTA:SPPO13:Firpic:Ir(ppy)₃:Ir(piq)₂acac. The inset in (b) shows the normalised PL and EL spectra obtained from the red SM-OLEDs studied here.

summarised in Table 1.

Next, we fabricated and investigated red SM-OLEDs including multiple-H-dip-coated EMLs (80 nm) with a co-mixed TCTA:SPPO13 host and co-mixed guest phosphors of Firpic:Ir(ppy)₃:Ir(piq)₂acac. Figure 8 shows the AFM morphologies of H-dip-coated EMLs of red-emitting TCTA:SPPO13:Firpic:Ir(ppy)₃:Ir(piq)₂acac deposited onto flat substrates with different numbers of H-dip-coating cycles. Similar to the blue- and green-emitting EMLs, the small molecular EMLs of TCTA:SPPO13:Firpic:Ir(ppy)₃:Ir(piq)₂acac fabricated by spin-coating and single H-dip-coating also show a surface morphology with many sub-micron-sized pinhole defects and relatively high surface roughness levels (*ca.* 0.67 nm). On the other hand, in contrast to the single-H-dip-coated EMLs, the multiple-H-dip-coated red EMLs are of a good film quality. The RMS surface roughness levels of the EMLs fabricated by double H-dip-coating and triple H-dip-coating were found to be *ca.* 0.43, and 0.31 nm, respectively.

We also investigated the *J-L-V* characteristics of multiple-H-dip-coated red SM-OLEDs, as shown in Fig. 9. For all of the OLEDs, the sharp slopes of the *J-V* curves indicate excellent diodic behaviours of the H-dip-coated EMLs. It is also clear that the charge injections are below 4.5–5.5 V, with sharp increases in the *J-L-V* curves. For example, the operating voltage of a red SM-OLED with a single-H-dip-coated EML is about 8.5 V for a brightness of 100 cd m⁻². In addition, these values are 11.0 V for 1,000 cd m⁻² and 17.5 V for 10,000 cd m⁻², with the luminescence reaching *ca.* 13,000 cd m⁻² (at 20.5 V). The figure also shows that the red EL brightness increases significantly in the devices with the multiple-H-dip-coated EMLs; the operating voltage of the green device with the triple-H-dip-coated EML is approximately 7.2 V for a brightness of 100 cd m⁻², while these values are 10.0 V for 1,000 cd m⁻² and 16.0 V for 10,000 cd m⁻², with the luminescence in this case reaching *ca.* 15,000 cd m⁻² (at 19.0 V). These values are much higher than those of the device with the single-H-dip-coated EML. Moreover, the efficiency levels show significant increases when multiple-H-dip-coated EMLs are used. The best overall performance was obtained in the red device with the triple-H-dip-coated EMLs, with a peak *LE* of 5.7 cd A⁻¹ and a peak *PE* of 2.3 lm W⁻¹. The EQEs of the red device with the triple-H-dip-coated EML is 7.0%, which is also higher than those of the red devices with double-dip-coated EML (EQE = 6.6%) and the reference device with the single-H-dip-coated EML (EQE = 4.8%). These results also indicate that the device performance levels are significantly improved when multiple-H-dip-coated EMLs are used. The inset in Fig. 9(b) shows the normalised EL spectra (at 1,000 cd m⁻²) obtained from the red OLEDs. As shown in this figure, only single dominant peaks are observed at 615 nm for the red devices, corresponding to the emission from Ir(piq)₂acac.¹¹ The performance capabilities of the red devices studied here are summarised in Table 1.

By combining the foregoing AFM morphology results with the performance (*J-L-V*) data of the multiple-H-dip-coated SM-OLEDs (Figs. 4, 7, and 9), it becomes clear that triple coated EMLs are capable of bright and efficient EL performance levels

for all blue, green, and red EL emissions. These levels exceed those of single-H-dip-coated EMLs. This demonstrates that the use of multiple-H-dip-coated EMLs is a sensible option for solution-processable SM-OLEDs due to their high luminance and efficiency levels.

Large-area multiple-H-dip-coated R, G, and B SM-OLEDs

Finally, encouraged by the impressive results obtained from the SM-OLEDs based on the multiple-H-dip-coated blue, green, and red EMLs of SPPO13:TCTA:phosphors, we fabricated large-area solution-processable SM-OLEDs on 5 cm × 5 cm ITO-coated glass substrates using the triple H-dip-coating method in order to assess the processability of large-area SM-OLEDs. A photographic image of the fabricated device is shown in Fig. 10(a). Blue, green, and red EMLs were deposited in sequence laterally on a PEDOT:PSS pre-coated ITO glass substrate using the triple H-dip-coating method to produce blue, green, and red OLEDs with a pixel size of about 3.0 cm × 1.0 cm. Although the solution-processed small molecular EMLs in the SM-OLEDs were fully fabricated in air, the figure clearly shows that the SM-OLEDs produced are fairly luminous. Moreover, the low variation in the emission intensity in the emission areas implies a small variation in the thickness of the solution-coated EMLs. Furthermore, this low variation in the

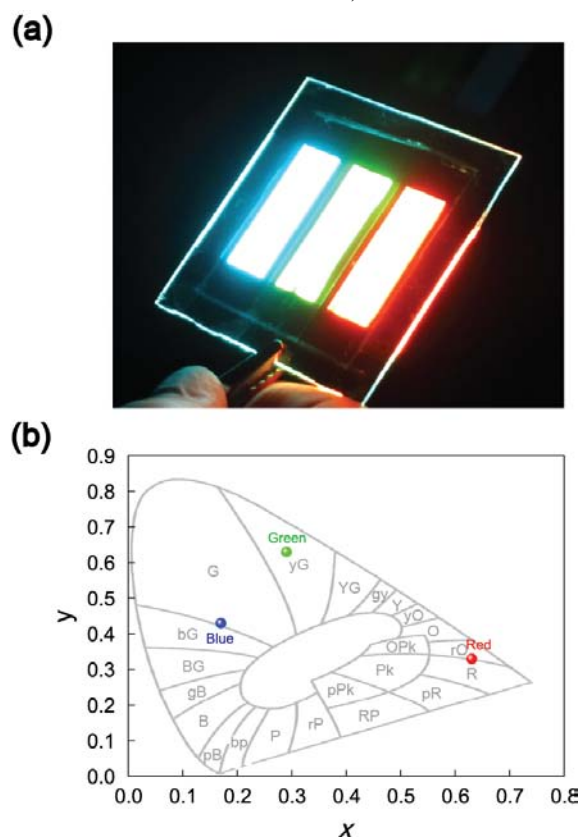


Fig. 10 (a) Photograph of operating solution-processable blue, green, and red SM-OLEDs at *ca.* 10.0 V on a 5 cm × 5 cm substrate, demonstrating the efficient EL properties of the multiple-H-dip-coated EMLs. (b) The 1931 CIE chromaticity diagram of the EL emissions from the SM-OLEDs studied here.

EL intensity over the active area provides evidence of the suitability of this method for large-scale fabrication. The EL spectra, collected from the pixels on the substrate, are nearly identical to those shown in Figs. 4, 7, and 9. As shown in Fig. 10(b), the blue-, green-, and red-emissive SM-OLEDs, exhibiting CIE coordinates of (0.15, 0.39), (0.28, 0.63), and (0.63, 0.33), respectively, at 1,000 cd m⁻², clearly show that with the introduction of multiple-H-dip-coated EMLs into OLEDs, one may easily obtain full-colour SM-OLEDs. These results clearly demonstrate that the multiple-H-dip-coating method for EMLs offers a bright and efficient fabrication process, with easy scaling up to larger sizes at lower costs compared to other processes. We want to note that the performance of the multiple-H-dip-coated SM-OLEDs could be further improved by selecting optimal host/guest materials, solvents, solution concentrations, viscosities, gap heights, and the number of coating cycles, among other parameters, and/or by combining the devices with additional functional layers such as hole-blocking or electron injecting layers, as reported in the literature.

In light of these observations, it is clear that the multiple-H-dip-coating process shows considerable promise for the production of flat, uniform, and large-area organic semiconducting layers, allowing the realization of rapidly processable and high-performance SM-OLEDs. Furthermore, the formation of small molecular functional layers by multiple H-dip-coating can also be put to good use in the fabrication of new electrical organic devices.

Conclusions

In summary, we successfully fabricated highly luminous, efficient, and large-area solution-processed small molecular OLEDs by incorporating multiple-H-dip-coated EMLs of TCTA:SPPO13:co-mixed phosphors. Blue, green, and red EL emissions were successfully demonstrated from the multiple-H-dip-coated EMLs. Maximum luminous efficiency levels of 15.8, 23.2, and 5.7 cd A⁻¹ were achieved for blue, green, and red EL emissions, respectively, which only decreased slightly to corresponding values of 13.7, 23.2, and 4.8 cd A⁻¹, even at a high luminance of 10,000 cd m⁻², without the use of a vacuum-evaporation process during the formation of the EMLs. These high luminance and efficiency levels contribute to the creation of high-quality film without the formation of nano-hole defects during the use of the multiple-H-dip-coating process. Blue, green, and red SM-OLEDs on a 5 cm × 5 cm substrate with high uniformity were also fabricated using the multiple-H-dip-coating process. In our study, we therefore show that EMLs fabricated using the multiple H-dip-coating process with a solution-processable co-mixed bipolar host:guest system can be used in high-performance full-colour SM-OLEDs and can furthermore be expanded to roll-to-roll coatings, which will facilitate the use of these devices in many applications, such as lighting, displays, and/or optoelectronic devices.

Acknowledgements

This work was supported by the Chungcheong Institute for the Regional Program Evaluation Promotion Project of the Korean Ministry of Knowledge Economy (R0001445) and by Kwangwoon University (2015). It was also supported by the Brain Korea 21 Project (2014).

Notes and references

Department of Electrophysics, Kwangwoon University, Seoul 139-701, Korea. Fax: +82-2943-3208; Tel: +82-2940-5237; E-mail: bcpark@kw.ac.kr

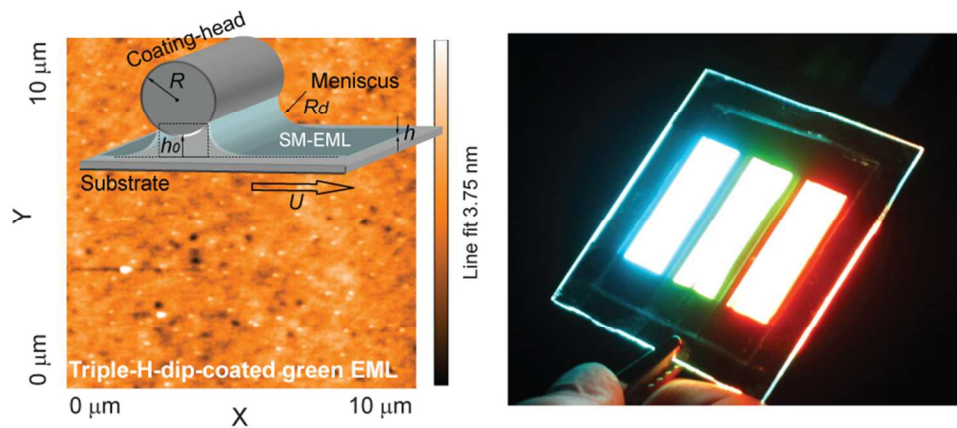
- 1 C. W. Tang and S. A. VanSlyke, *Appl. Phys. Lett.*, 1987, **51**, 913.
- 2 J. H. Burroughes, D. D. C. Bradley, A. R. Brown, R. N. Marks, K. Mackay, R. H. Friend, P. L. Burns and A. B. Holmes, *Nature*, 1990, **347**, 539-541.
- 3 M. A. Baldo, D. F. O'Brien, Y. You, A. Shoustikov, S. Sibley, M. E. Thompson and S. R. Forrest, *Nature*, 1988, **395**, 151-154.
- 4 M. A. Baldo, S. Lamansky, P. E. Burrows, M. E. Thompson and S. R. Forrest, *Appl. Phys. Lett.*, 1999, **75**, 4-6.
- 5 G. He, M. Pfeiffer, K. Leo, M. Hofmann, J. Birnstock, R. Pudzich and J. Salbeck, *Appl. Phys. Lett.*, 2004, **85**, 3911-3913.
- 6 Q. Wang, J. Ding, D. Ma, Y. Cheng, L. Wang, X. Jing and F. Wang, *Adv. Funct. Mater.*, 2009, **19**, 84-95.
- 7 G. He, O. Schneider, D. Qin, X. Zhou, M. Pfeiffer and K. Leo, *J. Appl. Phys.*, 2004, **95**, 5773.
- 8 N. Chopra, J. Lee, Y. Zheng, S.-H. Eom, J. Xue and F. So, *Appl. Phys. Lett.*, 2008, **93**, 143307.
- 9 Y. Tao, Q. Wang, C. Yang, Q. Wang, Z. Zhang, T. Zou, J. Qin and D. Ma, *Angew. Chem.*, 2008, **120**, 8224-8227.
- 10 L. Xiao, S.-J. Su, Y. Agata, H. Lan and J. Kido, *Adv. Mater.*, 2009, **21**, 1271-1274.
- 11 Y.-Y. Lyu, J. Kwak, W. S. Jeon, Y. Byun, H. S. Lee, D. Kim, C. Lee and K. Char, *Adv. Funct. Mater.*, 2009, **19**, 420-427.
- 12 S.-Y. Kim, W.-I. Jeong, C. Mayr, Y.-S. Park, K.-H. Kim, J.-H. Lee, C.-K. Moon, W. Brütting and J.-J. Kim, *Adv. Funct. Mater.*, 2013, **23**, 3896-3900.
- 13 Y. Hino, H. Kajii and Y. Ohmori, *Org. Electron.*, 2004, **5**, 265-270.
- 14 N. Rehmman, D. Hertel, K. Meerholz, H. Becker and S. Heun, *Appl. Phys. Lett.*, 2007, **91**, 103507.
- 15 L. Hou, L. Duan, J. Qiao, W. Li, D. Zhang and Y. Qiu, *Appl. Phys. Lett.*, 2008, **92**, 263301.
- 16 L. Duan, L. Hou, T.-W. Lee, J. Qiao, D. Zhang, G. Dong, L. Wang and Y. Qiu, *J. Mater. Chem.*, 2010, **20**, 6392-6407.
- 17 Q. Fu, J. Chen, C. Shi and D. Ma, *ACS Appl. Mater. Interfaces*, 2012, **4**, 6579-6586.
- 18 J. Chen, C. Shi, Q. Fu, F. Zhao, Y. Hu, Y. Feng and D. Ma, *J. Mater. Chem.*, 2012, **22**, 5164-5170.
- 19 Q. Fu, J. Chen, H. Zhang, C. Shi and D. Ma, *Opt. Express*, 2013, **21**, 11078-11085.
- 20 K. S. Yook and J. Y. Lee, *Adv. Mater.*, 2014, DOI: 10.1002/adma.201306266.
- 21 H. Liu, Q. Bai, L. Yao, D. Hu, X. Tang, F. Shen, H. Zhang, Y. Gao, P. Lu, B. Yang and Y. Ma, *Adv. Funct. Mater.*, 2014, **24**, 5881-5888.
- 22 H.-W. Chang, Y.-T. Lee, M.-R. Tseng, M.-H. Jang, H.-C. Yeh, F.-T. Luo, H.-F. Meng, C.-T. Chen, Y. Chi, Y. Qiu, L. Duan, H.-W. Lin, S.-F. Horng and H.-W. Zan, *Synthetic Metals*, 2014, **196**, 99-109.

- 23 B. Park and M. -Y. Han, *Opt. Express*, 2009, **17**, 21362-21369.
- 24 H. G. Jeon, Y. H. Huh, S. H. Yun, K. W. Kim, S. S. Lee, J. Lim, K. -S. An and B. Park, *J. Mater. Chem. C*, 2014, **2**, 2622-2634.
- 25 B. Park and M.-Y. Han, *Opt. Express*, 2009, **17**, 13830-13840.
- 26 H. G. Jeon, C. Y. Cho, J. C. Shin and B. Park, *J. Mater. Chem.*, 2012, **22**, 23022-23029.
- 27 B. Park, H. G. Jeon, J. Choi, Y. K. Kim, J. Lim, J. Jung, S. Y. Cho and C. Lee, *J. Mater. Chem.*, 2012, **22**, 5641-5646.
- 28 L. D. Landau and V. G. Levich, *Acta Physicochimica URSS*, 1942, **17**, 42-54.
- 29 Z. Wu, L. Wang, G. Lei and Y. Qiu, *J. Appl. Phys.*, 2005, **97**, 103105.
- 30 S. T. Lee, Z. Q. Gao and L. S. Hung, *Appl. Phys. Lett.*, 1999, **75**, 1404.
- 31 L. Ke, K. Zhang, N. Yakovlev, S.-J. Chua and P. Chen, *Mater. Sci. Eng. B*, 2003, **97**, 1-4.
- 32 A. Benninghoven, *Angew. Chem. Int. Ed. Engl.*, 1994, **33**, 1023-1043.

Table 1. Summary of device performance characteristics of SM-OLEDs based on multiple-H-dip-coated co-host (SPPO13:TCTA) : guest (Ir complexes) EMLs

Type	Coating cycles	L_{MAX} $cd\ m^{-2}$	LE_{MAX} $cd\ A^{-1}$	PE_{MAX} $lm\ W^{-1}$	At 1,000 $cd\ m^{-2}$		At 10,000 $cd\ m^{-2}$		CIE (x,y)
					LE $cd\ A^{-1}$	PE $lm\ W^{-1}$	LE $cd\ A^{-1}$	PE $lm\ W^{-1}$	
Blue	1	21,000	8.8	3.2	8.1	3.2	8.2	2.1	0.15, 0.39
	2	24,000	15.2	6.7	14.6	6.6	13.3	3.8	0.16, 0.42
	3	25,000	15.8	6.7	15.0	6.7	14.3	4.3	0.17, 0.43
Green	1	62,000	15.6	5.0	4.3	2.1	14.2	4.9	0.28, 0.63
	2	68,000	20.3	6.7	10.0	4.5	19.2	6.5	0.29, 0.63
	3	79,000	23.2	8.7	12.6	6.1	23.2	8.1	0.29, 0.63
Red	1	13,000	4.4	1.5	4.3	1.2	2.5	0.4	0.63, 0.33
	2	14,000	5.0	1.8	5.0	1.5	3.2	0.5	0.62, 0.33
	3	15,000	5.7	2.3	5.7	1.9	4.8	1.0	0.63, 0.33

OLED device structure: ITO/PEDOT:PSS HIL/EML /Cs₂CO₃/Al.



Small molecular organic light-emitting layers are successfully deposited by multiple horizontal-dip-coating to achieve highly bright and efficient solution-processable OLEDs.